Journal of Inflammation Research

Dovepress
open access to scientific and medical research

Open Access Full Text Article

ORIGINAL RESEARCH

Bushen Huoxue Formula Inhibits IL-1β-Induced Apoptosis and Extracellular Matrix Degradation in the Nucleus Pulposus Cells and Improves Intervertebral Disc Degeneration in Rats

Shang Gao[1], Chenmoji Wang[1], Lijie Qi[2], Songlin Liang[1], Xintian Qu[1], Wei Liu[3,*], Nianhu Li[4,*]

[1]The First Clinical Medical College of Shandong University of Traditional Chinese Medicine, Jinan, Shandong Province, People's Republic of China; [2]Qilu Hospital of Shandong University, Jinan, Shandong Province, People's Republic of China; [3]Shandong University of Traditional Chinese Medicine, Jinan, Shandong Province, People's Republic of China; [4]Affiliated Hospital of Shandong University of Traditional Chinese Medicine, Jinan, Shandong Province, People's Republic of China

*These authors contributed equally to this work

Correspondence: Nianhu Li; Wei Liu, Email tigerlee073@126.com; weiliu800109@163.com

Background: The method of action of Bushen Formula (BSHXF) in the treatment of intervertebral disc degeneration (IVDD) was uncovered in this work using in vivo and in vitro tests. To clarify the mechanism of action of BSHXF, we validated the rat intervertebral disc degeneration model and the nucleus pulposus cell degeneration model.

Methods: In an in vivo model of IVDD the study explores the impact of BSHXF on mitochondrial function, pro-inflammatory cytokines, pro-apoptotic factors, and matrix metalloproteinases. Additionally, it evaluates the induced degeneration of nucleus pulposus (NP) cells in an in vitro model stimulated by interleukin-1 β (IL-1β). The study measures the effects of BSHXF on both the inflammatory response and mitochondrial function.

Results: The MRI results showed that BSHXF reduced intervertebral disc volume reduction and degradation of NP tissue. HE, SO-FG and immunofluorescence further confirmed the protective effect of BSHXF on degenerative intervertebral discs. BSHXF reduced the inflammatory levels of IL-6 IL-1β and TNF-α in degenerative intervertebral disc tissue. Meanwhile, JC-1, mPTP and ROS detection revealed that BSHXF can restore mitochondrial function by regulating the expression of antioxidant proteins, playing a protective role in NP cells. Finally, the WB results showed that BSHXF can alleviate IL-1β mediate the degeneration of NP cells. BSHXF can alleviate NP cell apoptosis by inhibiting the expression of bax, cleaved caspase-3, caspase-3, and cyt-c, and increasing the expression of Bcl-2.

Conclusion: This study reveals that BSHXF inhibits the development of inflammatory factors, which may play a significant role in intervertebral disc degeneration. This implies that BSHXF is a suitable herbal medication for future research into inflammatory cytokine treatment.

Keywords: intervertebral disc degeneration, nucleus pulposus cell, BSHXF, apoptosis, inflammatory

Introduction

Intervertebral disc degeneration (IVDD) is a common spinal condition that profoundly affects patients' health and quality of life.[1,2] This prevalent musculoskeletal ailment is chronic and enduring, incurring substantial costs on individuals and the broader social economy while inflicting physical and psychological harm.[3,4] IVDD is a complex process believed to be caused by aging,[5,6] oxidative damage,[7,8] and changes in the intervertebral disc microenvironment.[9–11] Mechanical injuries locally disrupt the intervertebral disc microenvironment during the IVDD process, leading to tissue trauma and matrix remodeling.[12,13] Upon changes in the intervertebral disc microenvironment, there is a release and secretion of apoptotic factors, matrix metalloproteinases, and inflammatory factors.[14–16] The pathological mechanisms underlying

Received: 2 September 2023
Accepted: 27 December 2023
Published: 6 January 2024

disc degeneration, especially oxidative stress, apoptosis, extracellular matrix degradation, and inflammatory cascades, remain poorly understood.[17] NLRP3, a crucial component of the inflammasome, regulates and mediates inflammatory responses. Upon intervertebral disc damage or degeneration, intracellular NLRP3 activation may occur. These activated NLRP3 inflammasomes can induce the release of the pro-inflammatory cytokine IL-1β. IL-1β, a potent inflammatory mediator, not only promotes NLRP3 activation but also exacerbates the inflammatory response during intervertebral disc degeneration. This activation-triggered release of IL-1β by NLRP3 could initiate a destructive cycle, intensifying inflammatory damage to intervertebral disc tissue and potentially accelerating the degeneration process.[18,19] Earlier studies have linked the NLRP3 inflammasome to the inflammatory response in IVDD. Furthermore, endoplasmic reticulum (ER) stress, reactive oxygen species (ROS) damage, and NLRP3 inflammasome activation are all associated with IVDD.[20,21]

BSHXF is composed of five Chinese medicinal herbs, including Aconiti Lateralis Radix Praeparata, Rehmanniae Radix Praeparata, Radix Salviae, Morindae Officinalis Radix, and Curculiginis Rhizome. Interleukin-1 (IL-1) is a proinflammatory cytokine that a previous study indicated can be downregulated by BSHXF.[22] In clinical practice, BSHXF is commonly employed to address various conditions such as sciatica, lumbar disc herniation, and low back pain. BSHXF exhibits promising therapeutic potential and demonstrates a certain degree of preventive efficacy against IVDD. To establish a scientific basis for the clinical application of BSHXF in IVDD treatment, this study examined its protective effects on degenerative intervertebral discs through both in vivo and in vitro testing.

Materials and Methods

Preparation of the Bushen Huoxue Formula

BSHXF was composed of Aconiti Lateralis Radix Praeparata (10 g), Rehmanniae Radix Praeparata (20 g), Radix Salviae (20 g), Morindae Officinalis Radix (15 g), and Curculiginis Rhizome (10 g) as detailed in Table 1. These herbal components were procured from the pharmacy department of the affiliated hospital of Shandong University of Chinese Medicine in Jinan, China. They were verified by specialists from the school of pharmacy (Jinan, China). The origins, therapeutic components, and manufacturing procedures of BSHXF have been standardized to comply with The Chinese Pharmacopoeia 2015's specified compounds for enhanced quality control. Using a spinning evaporator, the herbs are blended and concentrated. The resultant BSHXF solution undergoes two rounds of filtration (0.22 m) and is heated for 30 minutes. These were sterilized and stored in a designated area at 4°C. The dosage levels were as follows: 35 mg/kg/d as the lowest dose, 70 mg/kg/d as the medium dose, and 140 mg/kg/d as the highest dose. Administration was conducted via gavage once daily at a rate of 1 mL per 100 g of body weight. Based on the standard formula for human and animal dosages, this dose in rats equated to 6.25 times the human equivalent dose.

Animals

Sprague-Dawley rats, aged 12 weeks and weighing 200±20g, were procured from Beijing Huafukang Biotechnology Co. The rats were housed under controlled conditions of (22±2)°C temperature, (50±20%) humidity, and a 12h/12h light/dark cycle. They were provided unrestricted access to the same specific pathogen-free (SPF) standard food and water. All experimental protocols adhered to the guidelines set by the Animal Ethics Committee of the Affiliated Hospital of Shandong University of Traditional Chinese Medicine.

Table 1 BSHXF Constituents

Scientific Name	Herb Name	Dosage (g)
Aconiti Lateralis Radix Praeparata	Fuzi	10
Rehmanniae Radix Praeparata	Shudi	20
Radix Salviae	Danshen	20
Morindae Officinalis Radix	Ba Jitian	15
Curculiginis Rhizome	Xianmao	10

Establishment of Rat IVDD Model and Treatment

All rats were randomly sorted into 5 groups: the control group (CG), model group (MG), low-dose BSHXF group (LBG), middle-dose BSHXF group (MBG), and high-dose BSHXF group, each comprising 6 rats. Prior to a 40 mg/kg intraperitoneal injection of 2% pentobarbital, the rats' weights were recorded. Following the identification of the tail discs (CO7/8) adjacent to the coccyx vertebra using palpation, as detailed in a previous study,[23] a 20G needle (4 mm in length) was inserted perpendicularly through the skin into the annulus fibrosus (AF) layer of the tail. Each needle was rotated 360 degrees for 45 seconds.

Medical Treatment

Following surgery, all rats were provided care and feeding at the Experimental Center of The Affiliated Hospital of Shandong University of Traditional Chinese Medicine. Rats in the control and model groups received normal saline therapy. Rats in the BSHXF group were administered varying dosages of BSHXF: a low dose (35 mg/kg body weight), a medium dose (70 mg/kg body weight), and a high dose (140 mg/kg body weight), via intragastric administration. The administration continued until the rats were euthanized. Throughout the experiment, all animals received attentive care and were allowed unrestricted movement and loading.

Magnetic Resonance Imaging (MRI) Examination

Four weeks post-surgery, all rats underwent a 3.0T (7.0 T/20 cm) MRI scan while under isoflurane anesthesia. The T2-mapped imaging sequence parameters were configured as follows: a 180° reversal angle, a repetition time of 2000 ms, a 6.00/3.00 cm field of view, and a fast spin echo sequence with an echo time of 36 ms.[24] This imaging sequence is commonly employed to depict water molecule movement within the extracellular matrix of collagen and proteoglycan. The magnetic resonance imaging T2 mapping results were analyzed using Image J.

Histological Evaluation

The tissue underwent PBS washing and was subsequently fixed in 4% formaldehyde for 12 hours. Following this, the disc underwent decalcification using 10% formic acid, gradual dehydration in ethanol, and eventual embedding in paraffin. The resulting tissue samples were 5 μm in thickness. For histological examination, each section was dewaxed, rehydrated, and stained using hematoxylin and eosin (H&E). This process enabled the identification and assessment of histological changes in IVDD, employing a predefined scale ranging from 5 to 15. This scale denotes the spectrum from mildly regressive IVDD to significantly regressive IVDD.[25]

SO-FG Staining

The samples underwent fixation using 4% paraformaldehyde, followed by decalcification and preparation into paraffin sections. After dewaxing and differentiation in acidic ethanol, staining commenced using the solid green dyeing solution for 5 minutes, succeeded by immersion in Safranin O dyeing solution for an additional 2 minutes. Subsequently, the sample underwent cleaning with an acetic acid solution to eliminate any residual solid green staining solution. Finally, the sample was sealed and photographed for analysis.

Alcian Blue

The paraffin sections underwent a 30-minute baking process at 65°C and subsequent dewaxing using xylene. Following this, a gradient ethanol hydration was performed before staining with Alcian blue. After another round of dehydration with gradient ethanol, the film was sealed and photographed under the microscope.

Immunohistochemical Analysis

Tissue slices were subjected to a semi-quantitative assessment of ADAMTS-4, MMP-9, and MMP-13 levels. Following paraffin section dewaxing, antigen repair, endogenous peroxidase block, and BSA block (1:200), primary antibodies (ADAMTS-4 1:100, MMP-9 1:100, and MMP-13 1:100) were incubated overnight with goat anti-mouse secondary

antibody at 4°C. Subsequently, nuclei were restained, dehydrated, and subjected to DAB staining. The analysis of images and microscopic examination concluded the process.

Immunofluorescence

Paraffin sections or cell slides, after dewaxing, underwent antigen repair and were blocked with bovine serum albumin (BSA). Following this, primary antibodies (Aggrecan 1:500, MMP9 1:500, MMP13 1:500, Collagen II 1:500, NLRP3 1:500) were applied. Subsequently, goat anti-rabbit secondary antibody was incubated at 4°C for 1 hour. DAPI was utilized to counterstain the nuclei. The sections were observed and captured using a fluorescent microscope.

Enzyme-Linked Immunosorbent Assay

Interleukin-1β (IL-1β), interleukin-6 (IL-6), and tumor necrosis factor-α (TNF-α) expression levels were quantified using an ELISA kit (Beyotime) following the manufacturer's guidelines. The process involved disc tissue dissection, centrifugation, and extraction of the supernatant. Subsequently, the expression levels of IL-1β, IL-6, and TNF-α were determined using an ELISA kit from Beyotime in China, adhering to the manufacturer's instructions.

Extraction and Culture of Rat NP Cells

The disc tissue was washed three times with phosphate-buffered saline (PBS) before being sliced into one cubic centimeter pieces. These tissue pieces underwent a 30-minute soaking in 0.25% trypsin digestion followed by a 4-hour incubation in 0.2% type II collagenase to yield NP cells. The resulting cell suspension was passed through a 200 μm colander and washed twice with PBS. Subsequently, a 37°C incubator with 5% CO_2, a 15% fetal DMEM/F12 recovery cell bovine serum, 100 mg/mL streptomycin, 100 U/mL penicillin, and 1% L-glutamine was utilized. Once the cells reached 85–90% confluence, they were trypsinized and cultivated on petri plates. The third-generation nucleus pulposus cells were utilized for further experimentation.

Detection of NP Cell Proliferation by CCK-8

Using a CCK-8 kit, the survival rates of NP cells in each group were assessed. Third-generation NP cells were collected and seeded at a density of 8×10^3 cells per well in a 96-well culture plate, then incubated for 24 hours at 37°C with 5% CO_2. BSHXF sera at concentrations of 0, 5%, 10%, 15%, 20%, and 25%, along with 50 ng/mL IL-1β,[26] were prepared. Each well, excluding the control, received 100 μL of the IL-1β solution, while the control wells were supplemented with 100 μL of complete medium containing 10% SD rat blank serum. After 24 hours of incubation, 10 μL of CCK-8 solution was added to each well, followed by an additional 4 hours of incubation. Subsequently, the absorbance of each well was measured at 450 nm using a microplate reader.

Determination of Reactive Oxygen Species (ROS)

ROS detection kits were employed to assess the concentrations of ROS in the NP cells. Following treatment, the NP cells underwent three rinses with PBS. Subsequently, the cells were exposed to 2.2',7'-dichlorodihydrofluorescein diacetate (DCFH-DA: 10 μM) and incubated for 25 minutes at 37°C. The intensity of intracellular ROS fluorescence was measured using confocal laser microscopy.

Mitochondrial Membrane Potential (Δψm)

Mitochondrial membrane potential (Δψm) in isolated nucleus pulposus (NP) cells (8×10^3 cells/well) was evaluated following the guidelines provided by the mitochondrial membrane potential assay kit (40752ES60, Yeasen, China). Red fluorescence (Ex 540 nm/Em 590 nm) indicates JC-10 aggregates, while green fluorescence (Ex 490 nm/Em 525 nm) indicates JC-10 monomers. The Δψm of each group was determined as the ratio of JC-10 aggregates to monomers.

Measurement of Lactate Dehydrogenase (LDH) and ATP Level

The ATP activity and lactate dehydrogenase (LDH) levels in the NP cells were measured using colorimetric kits for adenosine 5′-triphosphate (ATP) (Beyotime) and LDH (Beyotime), following the manufacturer's protocols. After

subjecting the NP cells to a 24-hour treatment with 50 ng/mL IL-1β, they were exposed to BSHXF-containing sera and then incubated at 37°C with 5% CO_2. Subsequently, the cells were collected and homogenized in 500 μL. The supernatant was collected to assess ATP and LDH levels.

Evaluation of Oxidative Stress

Catalase (CAT), glutathione peroxidase activity (GSH-Px), superoxide dismutase (SOD), malondialdehyde (MDA), and total antioxidant capacity (T-AOC) were assessed using the Nanjing Jiancheng Kit.

Real-Time Quantitative Polymerase Chain Reaction

Total RNA was extracted from NP cells in different treatment groups following the kit's guidelines. Subsequently, the RNA was reverse transcribed to generate cDNA. RT-qPCR analysis employed primers targeting collagen type II, aggrecan, caspase-3, MMP-9, MMP-13, and ADAMTS-5. GAPDH was used as the internal reference (refer to Table 2).

Western Blot Analysis

Western blotting was employed to assess the expression levels of ADAMTS-5, MMP-9, Cleaved-caspase-3, Caspase-3, Bcl-2, Cyt-c, and Bax. After lysing different NP cells in radioimmunoprecipitation assay (RIPA) buffer for 30 minutes, total protein was extracted. The protein concentrations were measured using a bicinchoninic acid (BCA) protein detection kit. Equal protein quantities were separated via SDS-PAGE, transferred to a nitrocellulose membrane, and incubated overnight at 4°C with primary antibodies targeting ADAMTS-5(1:250; No.41037; Abcam), MMP-9(1:1000; No.228402; Abcam), Cleaved-caspase-3(1:1000; No.9964; CST), Caspase-3 (1:2000; No.184787; Abcam), Bcl-2 (1:2000; No.182858; Abcam), Cyt-c (1:5000; No.13504; Abcam), Bax (1:5000; No.32503; Abcam), and GAPDH (1:5000; No.8245; Abcam). Following three rinses with TBST, the membrane was exposed to a secondary antibody, pre-diluted with horseradish peroxidase (HRP), for an hour at room temperature. Subsequently, the membrane underwent three 10-minute TBST rinses. Target band images were obtained using enhanced chemiluminescence (ECL) in a gel imaging system, with GAPDH serving as the internal reference.

Table 2 Primers Used in RT-qPCR

Name	Primer	Sequence
Collagen II	Forward	GAACTGGTGGAGCAGCAAGA
Collagen II	Reverse	AGCAGGCGTAGGAAGGTCAT
Aggrecan	Forward	GCGATGCCACCTTGGAAATC
Aggrecan	Reverse	AGTCCAGTGTGTAGCGTGTG
Caspase-3	Forward	AGCATGAAAGGGTGGTCTCA
Caspase-3	Reverse	GTCGGCATACTGTTTCAGCA
MMP-9	Forward	CGTCTTCCAGTACCGAGAGAAAGC
MMP-9	Reverse	CTTGGTCCACCTGGTTCAACTCAC
MMP-13	Forward	GTGACAGGAGCTAAGGCAGA
MMP-13	Reverse	AGCATGAAAGGGTGGTCTCA
ADAMTS-5	Forward	TTGTGAGTGAGACTGTGCGG
ADAMTS-5	Reverse	AACCTGCCTATGTTCCCTGC
ADAMTS-4	Forward	AGAGTCCTGCCAGCGGTCAAG
ADAMTS-4	Reverse	TCTGCCACCACCAGTGTCTCC
NLRP3	Forward	AAAGGAAGTGGACTGCGAGA
NLRP3	Reverse	TTCAAACGACTCCCTGGAAC
GAPDH	Forward	TCACGACCATGGAGAAGGCT
GAPDH	Reverse	CAGGAGGCATTGCTGATGATC

Statistical Analysis

Statistical analysis was performed using GraphPad Prism 8.0 (GraphPad, San Diego, CA). Data is expressed as mean ± SD. ANOVA (univariate or bidirectional) and Tukey's multiple comparison test were employed to compare different groups. Statistical significance was considered at $P < 0.05$.

Results

BSHXF Treatment Alleviates IVDD in IVDD Model Rats

T2-weighted MRI signals are indicative of disc degeneration severity (Figure 1A). The MRI findings indicated a notably lower signal intensity in the IVDD group compared to the control group. Nevertheless, post-treatment with BSHXF, the degree of IVDD markedly decreased in a dose-dependent manner, with the high dose of BSHXF displaying the most effective inhibition (Figure 1B).

BSHXF Inhibited Degradation of Nucleus Pulposus in IVDD Model Rats

The HE staining results provided a clear depiction of the morphology and structure of intervertebral discs across the groups. In the control group, the intervertebral disc structure remained intact, comprising a rounded and evenly distributed nucleus pulposus, neatly arranged and distinct from the annulus fibrosus. Conversely, in the model group, the disc structure appeared distorted, with the central nucleus pulposus absent and replaced by proliferative connective tissue, blending with the annulus fibrosus. However, after four weeks of BSHXF treatment, a notable improvement in disc structure and morphology was observed in a dose-dependent manner. SO-FG and Alcian Blue corroborated the HE staining findings. These results indicate that BSHXF effectively ameliorates histopathological degeneration of the intervertebral disc (Figure 2A–D). MMP-9, MMP-13, and ADAMTS-4 are key enzymes involved in extracellular matrix degradation in the nucleus pulposus, influencing the extracellular matrix breakdown. Immunohistochemistry (IHC) demonstrated significantly elevated expression of MMP-9, MMP-13, and ADAMTS-4 in the MG group compared to the CG group. However, in the LBG, MBG, and HBG groups, there was a significant dose-dependent decrease in the expressions of these enzymes (Figure 2E–H). RT-qPCR results aligned with IHC, revealing increased expressions in MG

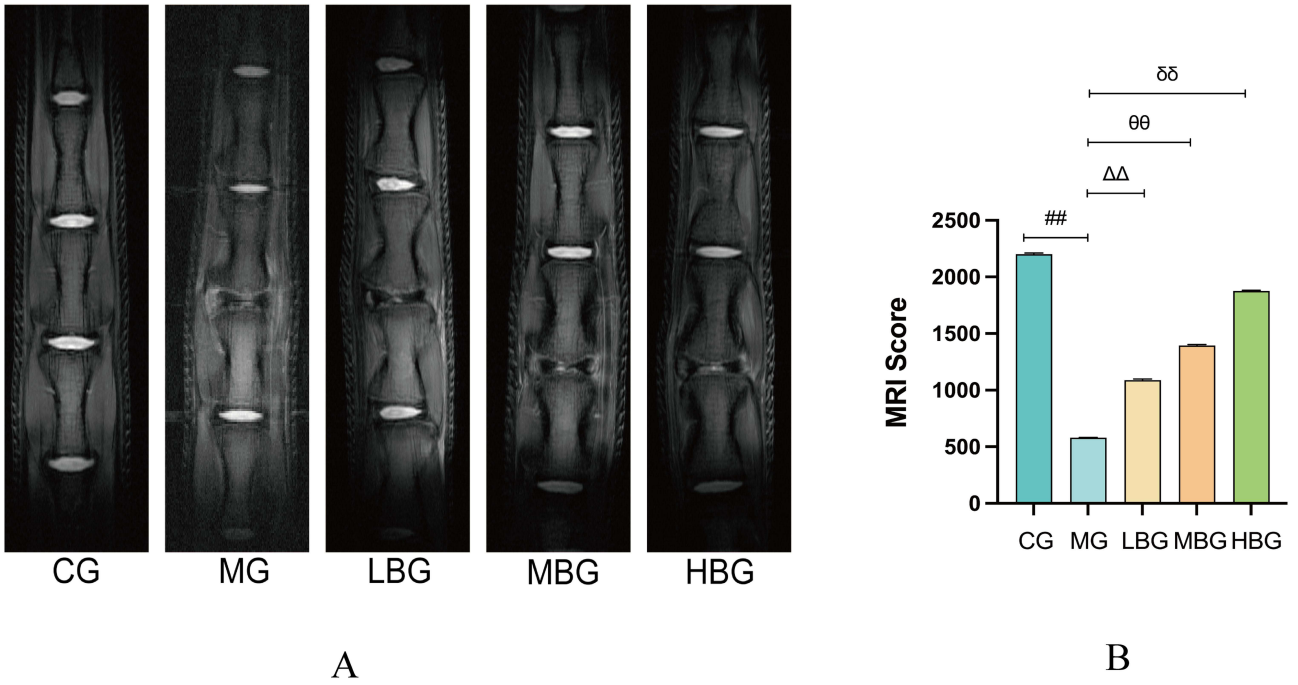

Figure 1 BSHXF improves the morphology and structure of intervertebral disc tissue. (**A** and **B**) T2-weighted MRI was used to detect intervertebral disc tissue. Data are means ± SD. ($^{\#\#}P < 0.01$; $^{\Delta\Delta}P < 0.01$; $^{\theta\theta}P < 0.01$; $^{\delta\delta}P < 0.01$).

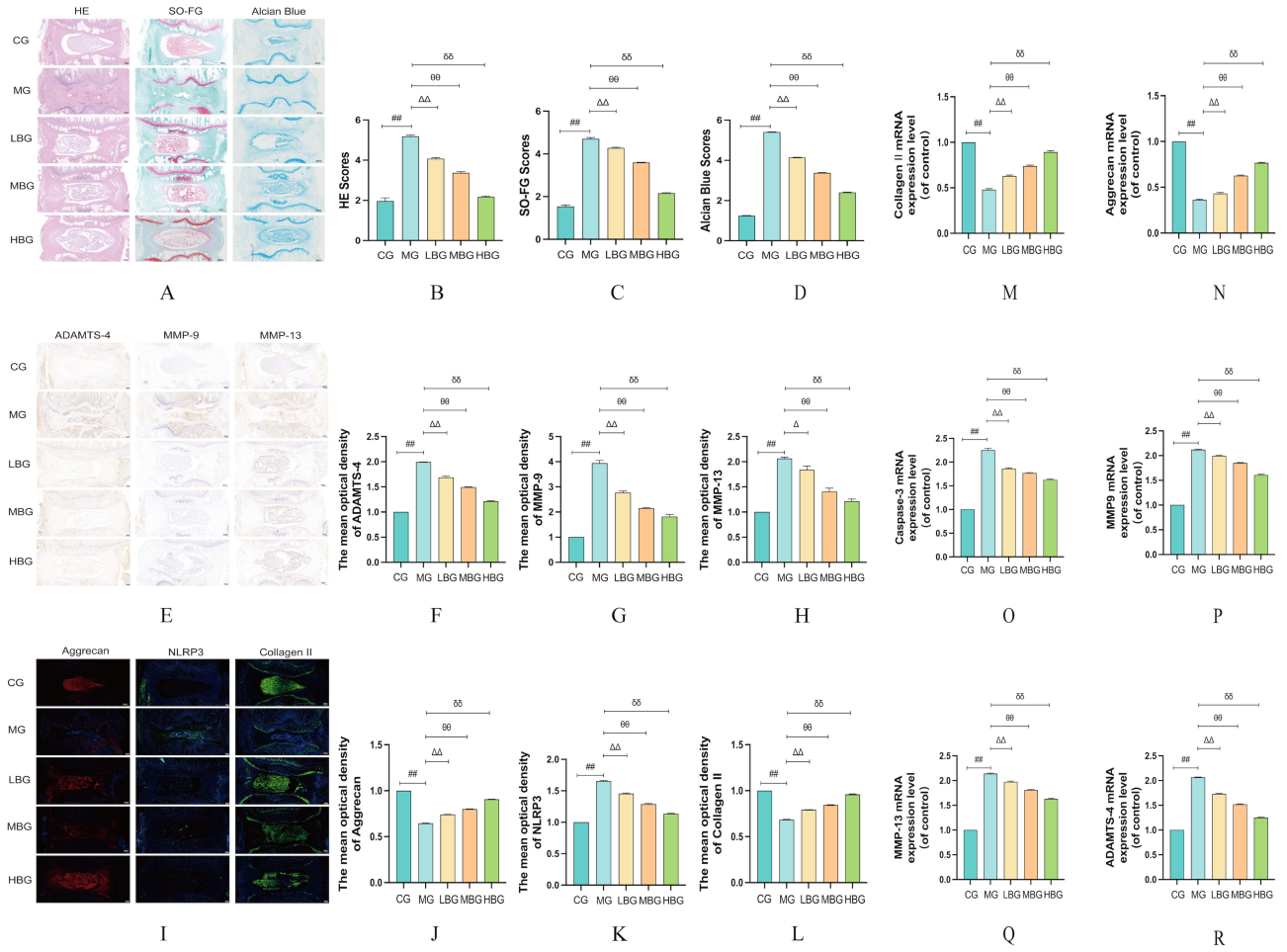

Figure 2 BSHXF Inhibited degradation of nucleus pulposus in IVDD model Rats. (**A**) HE staining, SO-FG and Alcian Blue. (**B**) The HE scores. (**C**) The SO-FG scores. (**D**) The Alcian Blue scores. (**E**) Immunohistochemistry of ADAMTS-4, MMP-9 and MMP-13. Immunofluorescence. (**F**) Immunohistochemistry of ADAMTS-4. (**G**) Immunohistochemistry of MMP-9. (**H**) Immunohistochemistry of MMP-13. (I) Immunofluorescence of Aggrecan, NLRP3 and Collagen II. (**J**) Immunofluorescence of Aggrecan. (**K**) Immunofluorescence of NLRP3. (**L**) Immunofluorescence of Collagen II. (**M–R**) The levels of collagen II, aggrecan, caspase-3, MMP-9, MMP-13 and ADAMTS-4 in intervertebral disc tissues were detected by RT-qPCR. Data are means ± SD.($^{\#\#}P < 0.01$; $^{\Delta\Delta}P < 0.01$,$^{\Delta}P < 0.05$; $^{\theta\theta}P< 0.01$; $^{\delta\delta}P< 0.01$).

and significant reductions post-BSHXF treatment. This suggests that BSHXF regulates the expression of MMP-9, MMP-13, and ADAMTS-4, contributing to intervertebral disc improvement (Figure 2P–R). In the MG, the fluorescence intensity of aggrecan and collagen II was notably lower than in the CG. Post-BSHXF treatment, there was a significant dose-dependent increase in fluorescence intensity, accompanied by mRNA levels showing reductions compared to CG but marked improvements in LBG, MBG, and HBG groups (Figure 2M and N). This demonstrates BSHXF's capacity to inhibit aggrecan and collagen II degradation, aiding in their recovery. Additionally, NLRP3 expression was significantly higher in the MG but significantly reduced after BSHXF treatment, evidencing the formula's capacity to effectively inhibit NLRP3 expression (Figure 2I–L). Moreover, RT-qPCR revealed increased caspase-3 expressions in the MG, notably mitigated following BSHXF treatment (Figure 2O).

BSHXF Alleviated Oxidative Stress in IVDD Model Rats

Cat, GSH-Px, T-AOC and LDH are classic measures of oxidative stress and test their ability to resist oxidative stress. The results of this study showed that the levels of Cat (Figure 3A and E), GSH-Px (Figure 3B and F) and T-AOC (Figure 3C and G) in serum and myeloid tissues of rats in the MG were significantly lower and the levels of LDH (Figure 3D and H) were higher compared to CG. After BSHXF treatment, the levels of Cat, GSH-Px and T-AOC in serum and nucleus pulposus tissues of rats tended to be higher and the levels of LDH were lower in a dose-dependent manner.

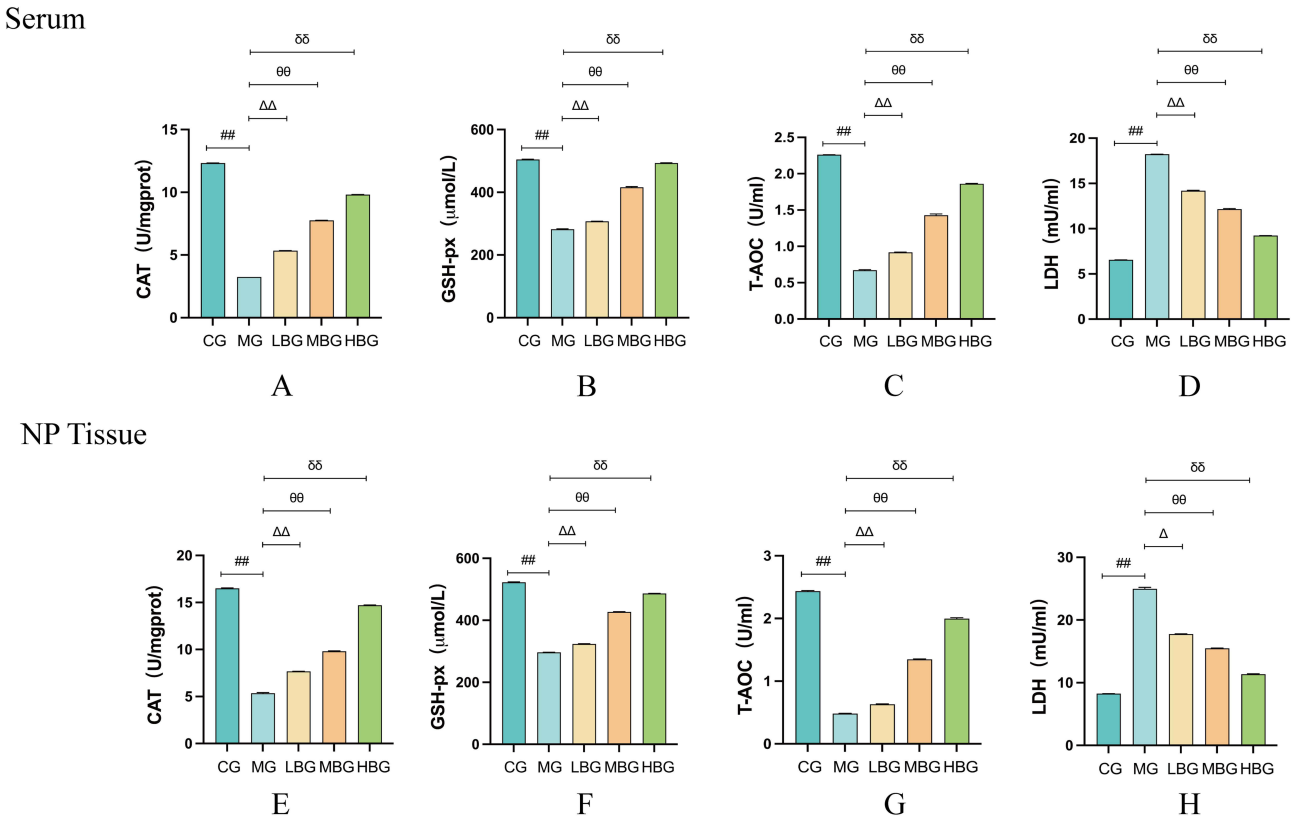

Figure 3 BSHXF alleviated oxidative stress in IVDD model Rats. (**A**–**H**) Assay of the oxidative capacity of CAT, GSH-px, T-AOC and LDH in rat serum and NP tissues. Data are means ± SD. ($^{\#\#}P < 0.01$; $^{\Delta\Delta}P < 0.01$,$^{\Delta}P < 0.05$; $^{\theta\theta}P< 0.01$; $^{\delta\delta}P< 0.01$).

BSHXF Alleviated Inflammation in IVDD Model Rats

As shown in Figure 4A–C, elisa results demonstrated that TNF-α, IL-6 and IL-1β levels in MG were significantly higher than those in CG. However, the expressions of TNF-α, IL-6 and IL-1β in LBG, MBG and HBG were significantly lower

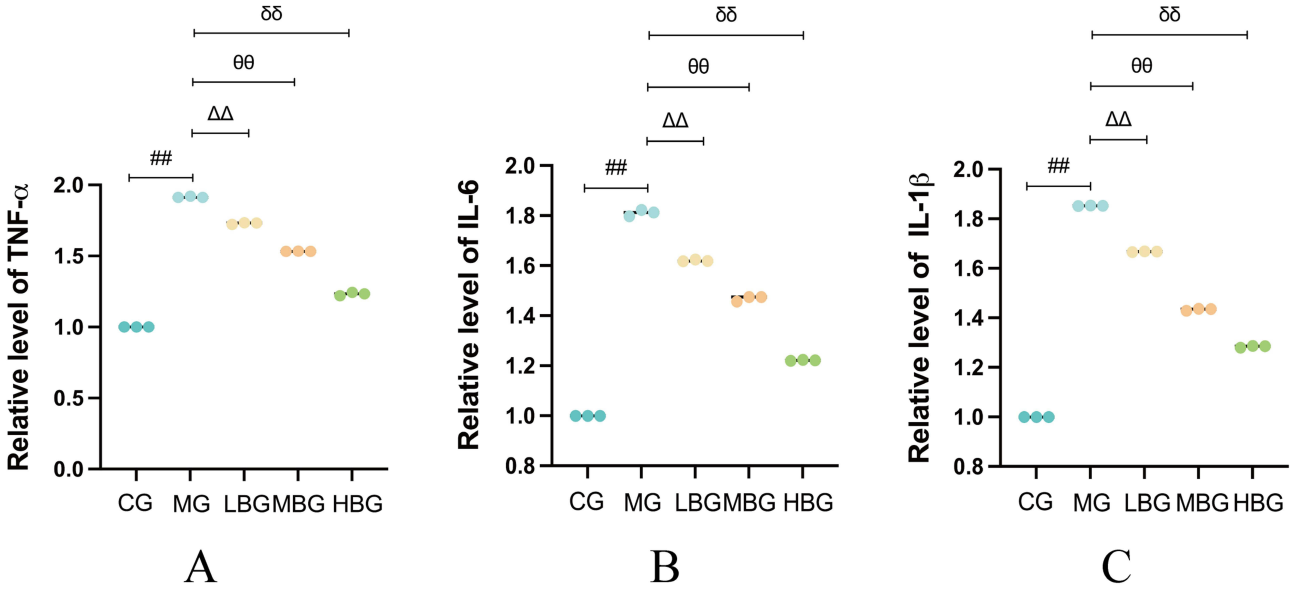

Figure 4 BSHXF alleviated inflammation in IVDD model Rats. (**A**–**C**) Measurement of TNF-α, IL-6 and IL-1β. Data are means ± SD.($^{\#\#}P < 0.01$; $^{\Delta\Delta}P < 0.01$; $^{\theta\theta}P< 0.01$; $^{\delta\delta}P< 0.01$).

than those in MG. These results suggest that BSHXF can improve IVD by inhibiting the expression of TNF-α, IL-6 and IL-1β.

Effect of BSHXF on NP Cell Viability

Normal NP cell morphology is shown in Figure 5A. NP cells were subjected to various concentrations of serum containing BSHXF (0, 5%, 10%, 15%, and 20%) for 24 h and then assayed with a CCK-8 kit. Sera containing BSHXF promoted NP cell proliferation in a dose-dependent manner and the optimal BSHXF concentration was 15% (Figure 5B and C). The NP cells were then exposed to 20 ng/mL IL-1β for 24 h followed by various doses of serum containing BSHXF for another 24 h. NP cell viability was markedly lower in the treatment than the control group. Relative to the IL-1β group, NP cell proliferation increased in the presence of serum containing BSHXF in a dose-dependent manner (Figure 5D).

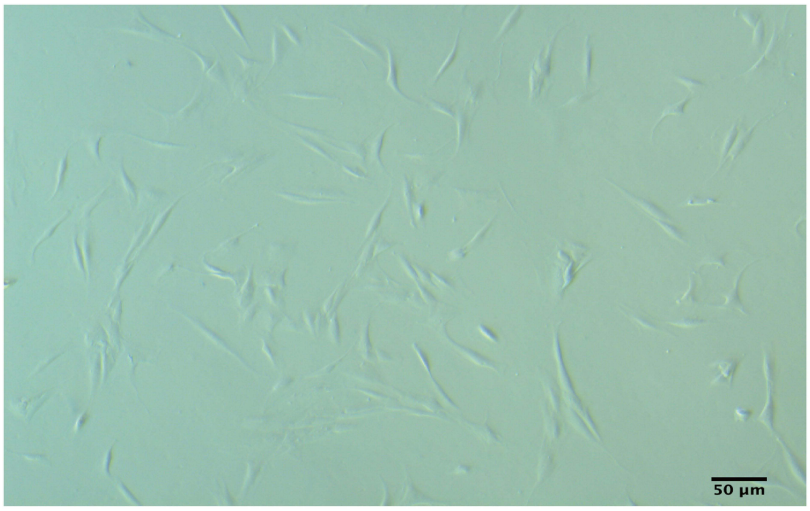

A

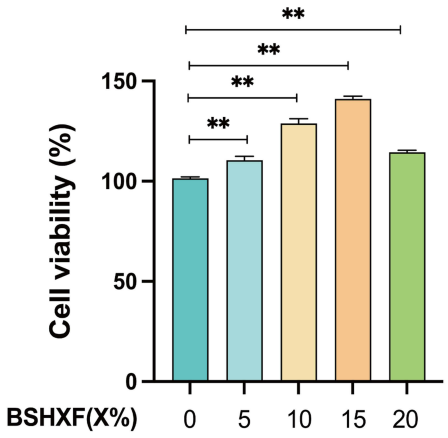

B

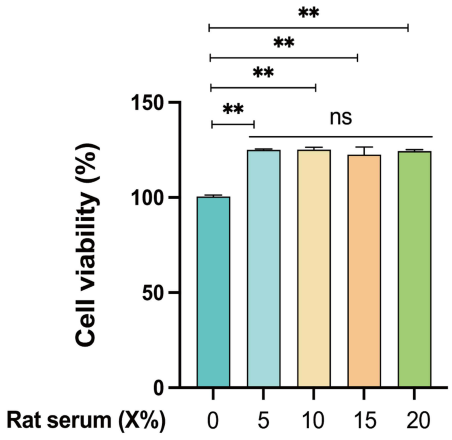

C

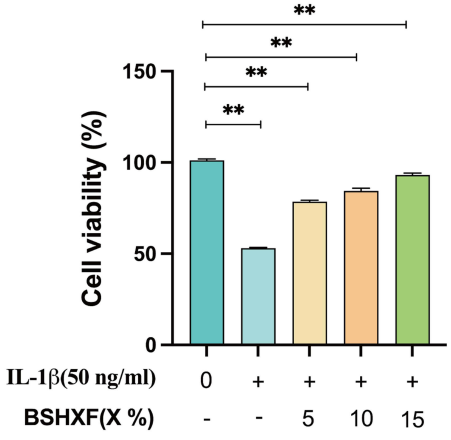

D

Figure 5 The protective effect of BSHXF on NP cells. (**A**) The morphology of NP Cell. (**B**) Effect of BSHXF on NP cell proliferation. (**C**) Effect of rat serum without BSHXF on NP cells. (**D**) Effect of IL-1β on NP cell proliferation. Data are means ± SD. (**P < 0.01).

Effect of BSHXF on Extracellular Matrix

Extracellular matrix degradation stands as a primary factor in IVDD. This degradation primarily arises from the overexpression of inflammatory factors. Markers indicative of extracellular matrix alterations were evaluated using Immunofluorescence, RT-qPCR, and Western blot analyses. Upon IL-1β induction, the fluorescence intensity of aggrecan (Figure 6A and B) and collagen II (Figure 6D and E) substantially decreased, yet exhibited increased intensity in the presence of BSHXF. Conversely, the fluorescence intensity of MMP-9 (Figure 6G and H), MMP-13 (Figure 6J and K), and NLRP3 (Figure 6M and N) notably heightened, but this phenomenon was reversed by BSHXF. The mRNA levels of aggrecan (Figure 6C) and collagen II (Figure 6F) in BSHXF-treated cells were notably higher than those in IL-1β-treated cells. However, the levels of MMP-9 (Figure 6I), MMP-13 (Figure 6L), NLRP3 (Figure 6O) and ADAMTS-5 (Figure 6S) were more pronounced in IL-1β-treated cells compared to those in BSHXF-treated cells. The Western blot data revealed that BSHXF downregulated the protein expression of ADAMTS-5 and MMP-9 induced by IL-1β (Figure 6P–R).

Effect of BSHXF on Mitochondrial Function

Mitochondrial dysfunction seriously affects cell energy supply and metabolism, leading to cell apoptosis. IL-1β disrupts the mitochondrial membrane potential, leads to mPTP inactivation and increases ROS activity. After BSHXF treatment, the membrane potential was gradually restored and mPTP function was significantly restored and reduced the accumulation of ROS (Figure 7A–C). The results of TEM showed that IL-1β disrupts mitochondrial morphology, causing swelling of the mitochondria and loss of the inner and outer membranes as to impair their function. Then after the treatment of

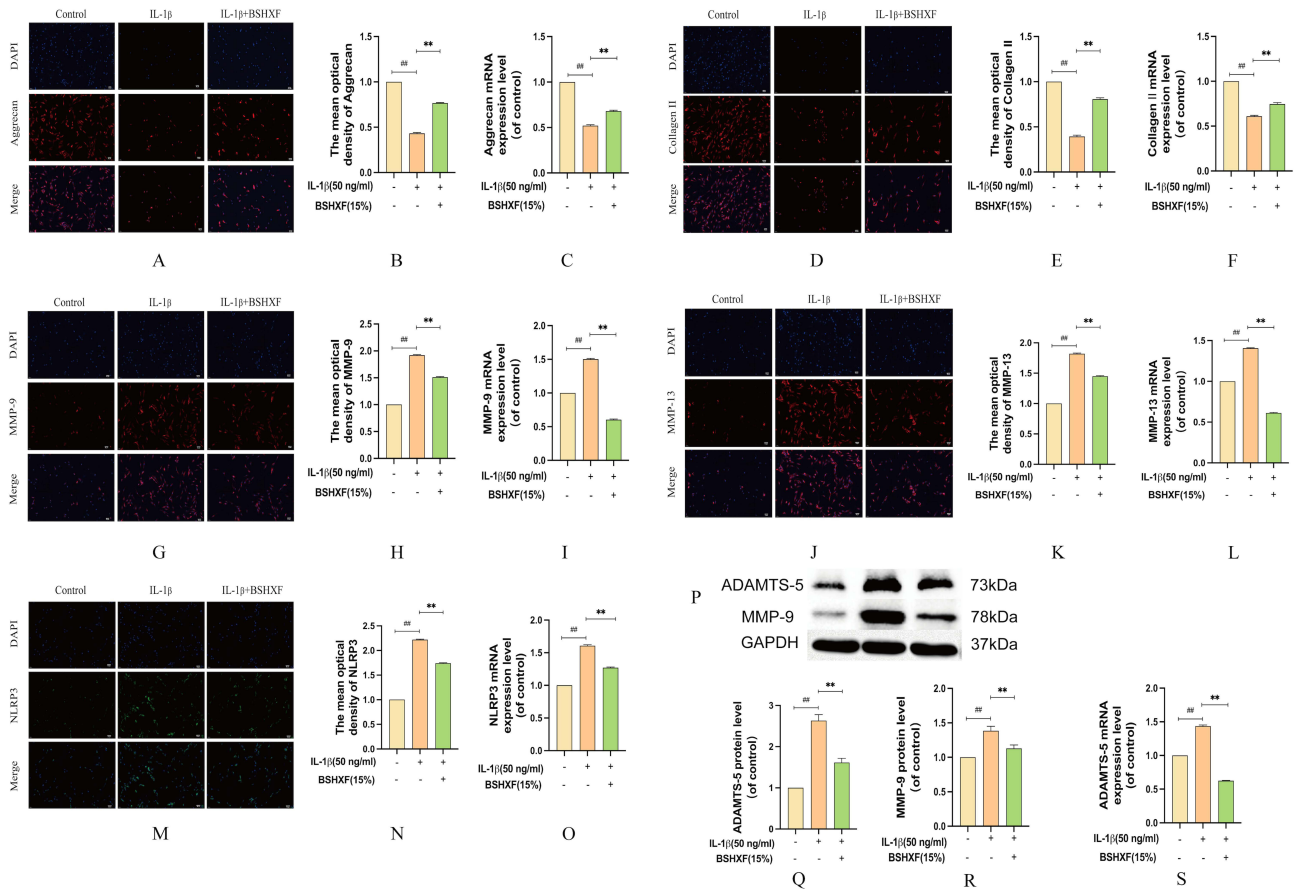

Figure 6 Effect of BSHXF on ECM induced by IL-1β. (**A** and **B**) Immunohistochemistry expression of aggrecan. (**C**) mRNA expression of aggrecan. (**D** and **E**) Immunohistochemistry expression of collagen II. (**F**) mRNA expression of collagen II. (**G** and **H**) Immunohistochemistry expression of MMP-9. (**I**) mRNA expression of MMP-9. (**J** and **K**) Immunohistochemistry expression of MMP-13. (**L**) mRNA expression of MMP-13. (**M** and **N**) Immunohistochemistry expression of NLRP3. (**O**) mRNA expression of NLRP3. (**P–R**) The protein expression of ADAMTS-5 and MMP-9. (**S**) mRNA expression of ADAMTS-5. Data are means ± SD. (**P < 0.01; ##P < 0.01).

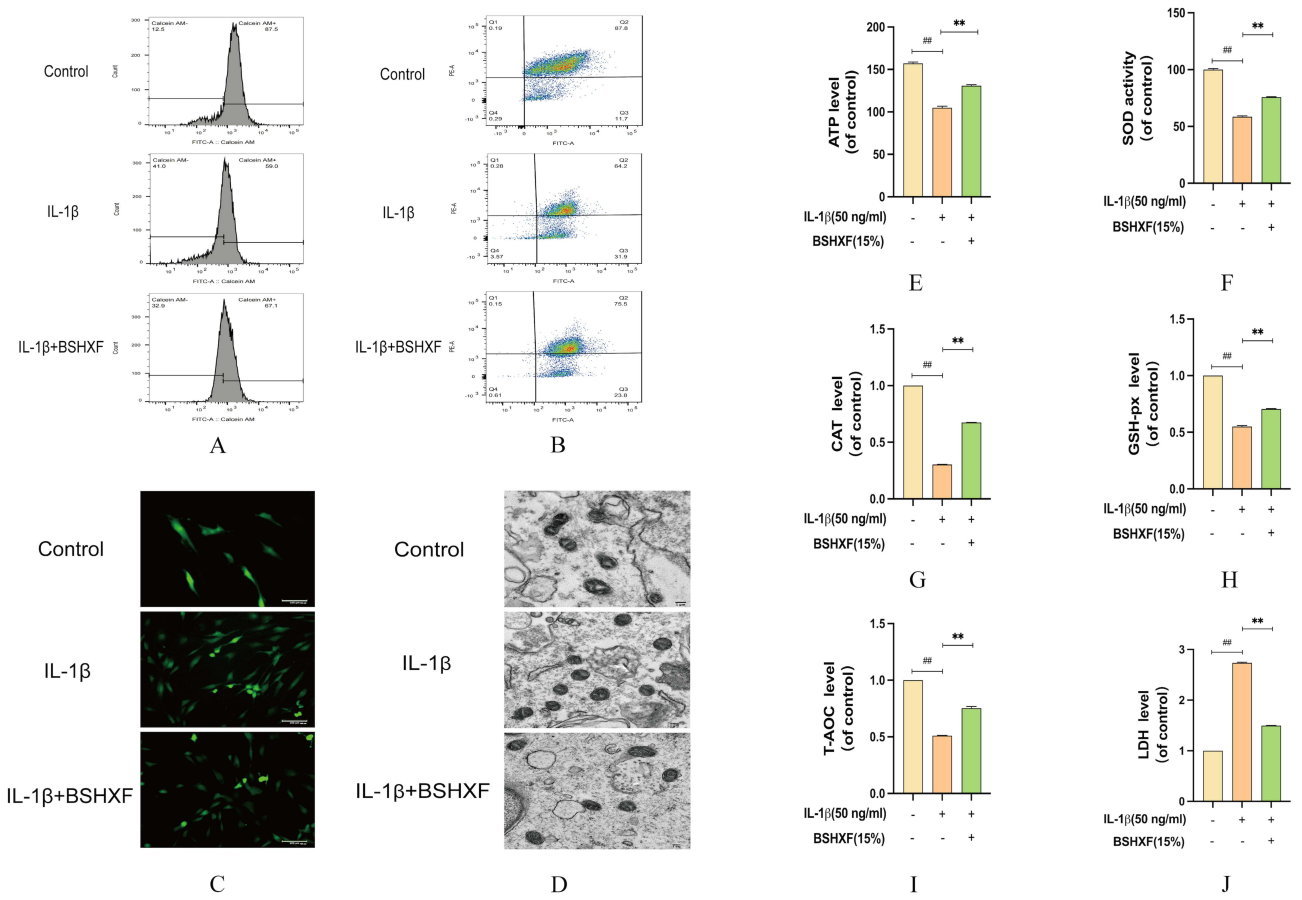

Figure 7 Effect of BSHXF on Mitochondrial function. (**A**) Detection of JC-1. (**B**) Detection of mPTP. (**C**) Effect of serum containing BSHXF on ROS level. (**D**) Detection of mitochondrial morphology. (**E**) Effect of serum containing BSHXF on ATP level. (**F**) Effect of serum containing BSHXF on SOD activity. (**G–J**) The oxidative capacity of CAT, GSH-px, T-AOC and LDH in NP cells. Data are means ± SD. (**P < 0.01; ##P < 0.01).

BSHXF, the opposite result appeared (Figure 7D). SOD and ATP were measured to detect mitochondrial function. After the NP cells were treated with IL-1β, SOD and ATP were depleted. However, BSHXF intervention increased the levels of SOD and ATP (Figure 7E and F). The oxidative capacity of NP cells showed that IL-1β significantly reduced the antioxidant capacity of CAT, GSH-px and T-AOC and increased the level of LDH (Figure 7G–J). However, the opposite result was observed after treatment with BSHXF. Hence, IL-1β promotes dysregulates ATP/SOD homeostasis and damages mitochondria oxidative capacity.

Effect of BSHXF on Apoptosis

Western blotting was employed to investigate the anti-apoptotic impact of BSHXF. In response to IL-1β treatment, both Bax c-caspase-3 and caspase-3 exhibited upregulated expression, while Bcl-2 demonstrated downregulation (Figure 8A–E). Conversely, BSHXF treatment exerted opposite effects. Additionally, assessment of relative cytochrome C protein expression levels across treatment groups indicated its translocation from mitochondria to the cytoplasm (Figures 8F and G). Using cell flow cytometry, the findings revealed that BSHXF exhibits the capability to suppress IL-1b induced apoptosis in nucleus pulposus cells (Figures 8H and I). These findings illustrate that IL-1β significantly induced apoptosis in NP cells, whereas BSHXF treatment inhibited apoptosis and fostered NP cell proliferation.

Discussion

In recent years, there has been a notable rise in the utilization of Traditional Chinese Medicine (TCM) therapies. Among these therapies, formulations like BSHXF have shown promising efficacy in addressing IVDD,[27] a syndrome

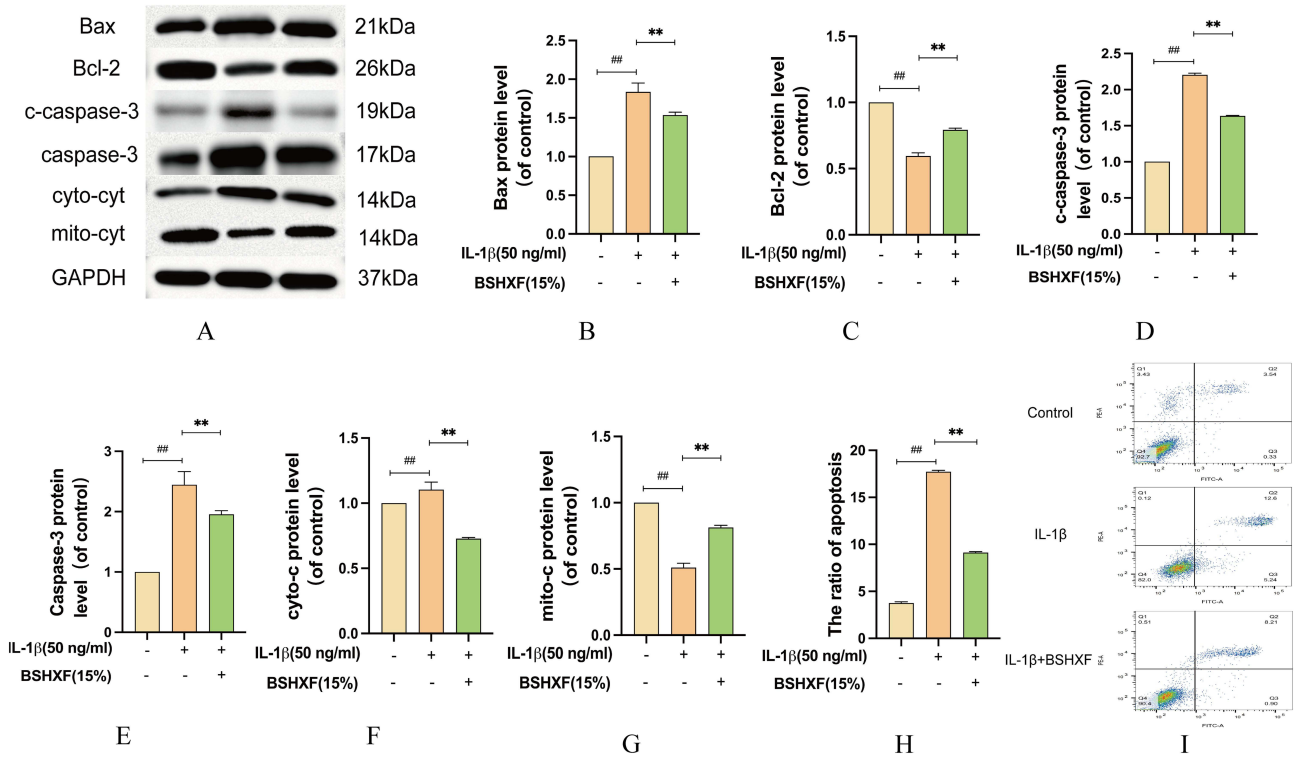

Figure 8 Effect of BSHXF on Cell. (**A**–**G**)The protein expression of Bax, Bcl-2, c-caspase-3, caspase-3, Cyt detected by Western blot. (**H** and **I**) Apoptosis by flow cytometry.(**P < 0.01; ##P < 0.01).

characterized by kidney deficiency and blood stasis. The prescribed approach involves herbal treatment aimed at nourishing the kidneys and enhancing blood circulation, both of which align with the functions performed by BSHXF.[28] TCM formulations comprise a blend of Chinese herbs, each with diverse effects within the composition-target network. This complexity poses challenges in understanding the individual therapeutic mechanisms of each component.[29] Despite its known efficacy, the specific molecular mechanisms underlying BSHXF's treatment of IVDD remain unclear. Therefore, this study delved into elucidating these mechanisms through a series of in vivo and in vitro experiments, aiming to pinpoint the interactions between its components and shed light on their modes of action.[30]

In our study, the experimental outcomes strongly indicate that disc degeneration primarily stems from the excessive production and infiltration of inflammatory factors. Factors like IL-6, IL-1β and TNF-αtrigger an overwhelming buildup of ROS within cells, disrupting their energy balance and wreaking havoc on crucial cellular functions.[23,31,32] BSHXF emerges as a pivotal agent in this scenario, enhancing mitochondrial functionality, regulating oxidative stress within NP cells, and reinstating cellular energy equilibrium. Consequently, it impedes IL-1β-induced apoptosis and the degradation of the extracellular matrix, exhibiting potent anti-apoptotic and antioxidant properties. These significant discoveries, validated through rigorous in vivo and in vitro experiments, offer fresh insights into the intricate molecular mechanisms through which BSHXF impacts IVDD. Elevated levels of inflammatory factors exacerbate the accumulation of ROS, instigating disruptions in mitochondrial functions, oxidative stress, and ultimately contributing to apoptosis in myeloid cells.

Hence, restoring mitochondrial function and effectively clearing accumulated ROS stand out as viable methods to enhance the functionality of myeloid nuclei.[33,34] Our findings indicate that inflammatory factors, particularly IL-1β, not only elevate ROS levels and impair mitochondrial function but also trigger apoptosis. Notably, IL-1β prompts an increase in ADAMTS levels within NP cells, notably ADAMTS-5, surpassing other ADAMTS in its induction. Our results underscore the upregulation of MMP-9, MMP-13, and ADAMTS-5 expression alongside a downregulation of type II collagen expression in IL-1β-induced cells. The surge in reactive oxygen amplifies intracellular Bax levels, hastens cytochrome c release from mitochondria, and intensifies the pace of apoptosis.

Concurrent studies suggest that heightened intracellular ROS levels might also induce the expression of matrix-degrading proteases.[35,36]

In cases of rheumatoid arthritis, beta-sitosterol showcases its efficacy by diminishing the concentration of inflammatory factors, bolstering the REDOX state, and demonstrating anti-arthritis effects. It achieves this by inhibiting NF-kB and activating the HO-1/Nrf-2 pathway.[37,38] Within BSHXF, Tanshinone IIA stands as a significant active component. Research has indicated its capacity to suppress the expression of inflammatory factors. Moreover, it curtails the buildup of active substances and mitigates cell apoptosis through its potent antioxidant properties.[39,40] Stigmasterol, a primary active compound found in Achyranthes bidentata, has demonstrated remarkable inhibition of proinflammatory factors and matrix degradation in chondrocytes. In our in vitro investigations, BSHXF notably reduced levels of key inflammatory factors like TNF-α and IL-6. It also suppressed the expression of enzymes associated with extracellular matrix breakdown, effectively mitigating extracellular matrix degeneration. Through RT-qPCR and Elisa analyses, we established a close correlation between NP apoptosis and several factors, including inflammatory mediators, apoptotic markers, and matrix metalloproteinases such as TNF-α, IL-6, caspase-3, MMP-9, MMP-13, and ADAMTS-5. Elisa results further confirmed that BSHXF decreased the secretion of TNF-α, IL-6, MMP-9, and MMP-13, despite their marked increase observed during disc degeneration. Additionally, our Western blot findings demonstrated that BSHXF inhibited the expression of MMP-9 and ADAMTS-5 amid disc degeneration. A wealth of prior research has solidified the crucial roles played by TNF-α, IL-6, caspase-3, and MMP-9 in the apoptosis of NP cells and the progression of IVDD.[41,42] These findings underscore the potential of BSHXF in modulating these pivotal factors, offering promising avenues for IVDD intervention.

Overall, our data indicates a cascade initiated by the over-secretion of inflammatory factors triggering an inflammatory response, culminating in the activation of NLRP3. This activation subsequently triggers the expression of caspase-3 and MMPs, ultimately leading to NP cell apoptosis and proteoglycan destruction. This process disrupts the structure of the annulus fibrosus, resulting in disarray. Furthermore, TNF-α concentration amplifies mir-660 expression, consequently elevating apoptosis rates and the expression of caspase-3 and caspase-7, thereby contributing to IVDD.[43] Moreover, our study reveals that under IL-1β stimulation, NP cells exhibit increased expression of pertinent inflammatory mediators (iNOS and COX-2) along with inflammatory cytokines (TNF-α and IL-6).[44] Our findings corroborate the deleterious effects of MMP-9 and MMP-13, which induce extracellular matrix degradation, morphological changes, structural disruption in NP tissue, alter its stress environment, and affect NP cell function. Additionally, our investigation elucidates the role of DNMT3B in modifying the TRPA1 promoter, thereby inhibiting COX2 expression through methylation. Overexpressed COX2 further promotes NP cell apoptosis. DNMT3B's promotion of NP cell proliferation via the TRPA1/COX2/YAP axis inhibits MMP-9 expression, preventing extracellular matrix degradation and ultimately reducing IVDD in rats.[45,46] Collectively, these studies present compelling evidence that BSHXF possesses anti-inflammatory, antioxidant, and extracellular matrix preserving properties. These attributes highlight its potential in addressing and potentially treating disc degeneration.We applied BSHXF to rats with disc degeneration and verified the link between BSHXF and IVDD in terms of molecular function and biological processes through in vivo experiments. In response to this treatment, the nucleus pulposus tissue recovered in a dose-dependent manner. Activation of NLRP3 inflammatory vesicles, induced by ROS, accelerated mitochondrial dysfunction and the release of pro-apoptotic factors, leading to apoptosis. As recognized in our study, TNF-α, IL-6, IL-1β and MMP-9 are core anti-inflammatory targets of BSHXF that have been validated by in vivo animal models. Therefore, BSHXF may be a potential herbal formulation for the treatment of IVDD.

While we have showcased BSHXF's promising therapeutic effects on disc degeneration, our next study aims to delve deeper into validating the mechanisms of action behind the main active ingredients within BSHXF concerning intervertebral disc degeneration.

Conclusion

In this study, we delved into understanding the mechanism behind BSHXF's efficacy in treating intervertebral disc degeneration through a series of in vivo and in vitro experiments. Our findings unveiled that BSHXF plays a pivotal role in enhancing mitochondrial function and morphology, reinstating energy balance, regulating oxidative stress, curbing

apoptosis, and mitigating matrix degeneration within the nucleus pulposus. Remarkably, it also fosters the recovery of nucleus pulposus tissue.

Data Sharing Statement

The datasets utilized or scrutinized during this study are accessible upon reasonable request from the corresponding author.

Ethics Approval and Consent to Participate

12-week-old male Sprague-Dawley rats were procured from Jinan Pengyue Animal Co., LTD. These animals were housed in the Laboratory Animal Center of the Affiliated Hospital of Shandong University of Chinese Medicine, ensuring a barrier environment at the SPF level. The experimental protocol involving animal research received approval from the Animal Ethics Committee of the Affiliated Hospital of Shandong University of Chinese Medicine, under the Ethics approval number: 2020-35.

Author Contributions

From designing the study to its execution, encompassing data collection and analysis, all authors have made substantial contributions to this manuscript; have been actively engaged in drafting, revising, and reviewing these provisions. Moreover, all authors have given their final approval for the forthcoming version, collectively agreeing to assume responsibility for all facets of the work.

Funding

Shandong Provincial Natural Science Foundation project (ZR202211240011); Key project of the Shandong Gerontological Society (LKJGG2021Z009); National Studio for Inheriting the Expertise of Renowned Traditional Chinese Medicine Practitioners - Xu Zhanwang (National Letter of Education on Traditional Chinese Medicine Practitioners [2022] No. 75).

Disclosure

The authors claim that they have no known competing financial interests or personal relationships that might affect this work.

References

1. Long J, Wang X, Du X, et al. JAG2/Notch2 inhibits intervertebral disc degeneration by modulating cell proliferation, apoptosis, and extracellular matrix. *Arthritis Res Ther*. 2019;21(1):213. doi:10.1186/s13075-019-1990-z
2. Yang S, Zhang F, Ma J, et al. Intervertebral disc ageing and degeneration: the antiapoptotic effect of oestrogen. *Ageing Res Rev*. 2020;57:100978. doi:10.1016/j.arr.2019.100978
3. Knezevic NN, Candido KD, Vlaeyen JWS, et al. Low back pain. *Lancet*. 2021;398(10294):78–92. doi:10.1016/S0140-6736(21)00733-9
4. Urits I, Burshtein A, Sharma M, et al. A comprehensive review: pathophysiology, diagnosis, and treatment. *Curr Pain Headache Rep*. 2019;23(3):23. doi:10.1007/s11916-019-0757-1
5. Novais EJ, Tran VA, Johnston SN, et al. Long-term treatment with senolytic drugs dasatinib and quercetin ameliorates age-dependent intervertebral disc degeneration in mice. *Nat Commun*. 2021;12(1):5213. doi:10.1038/s41467-021-25453-2
6. Silva MJ, Holguin N. Aging aggravates intervertebral disc degeneration by regulating transcription factors toward chondrogenesis. *FASEB J*. 2020;34(2):1970–1982. doi:10.1096/fj.201902109R
7. Cao G, Yang S, Cao J, et al. The role of oxidative stress in intervertebral disc degeneration. *Oxid Med Cell Longev*. 2022;2022:2166817. doi:10.1155/2022/2166817
8. Che H, Li J, Li Y, et al. p16 deficiency attenuates intervertebral disc degeneration by adjusting oxidative stress and nucleus pulposus cell cycle. *Elife*. 2020;9:e52570. doi:10.7554/eLife.52570
9. Che YJ, Guo JB, Liang T, et al. Assessment of changes in the micro-nano environment of intervertebral disc degeneration based on Pfirrmann grade. *Spine J*. 2019;19(7):1242–1253. doi:10.1016/j.spinee.2019.01.008
10. Che YJ, Hou JJ, Guo JB, et al. Low energy extracorporeal shock wave therapy combined with low tension traction can better reshape the microenvironment in degenerated intervertebral disc regeneration and repair. *Spine J*. 2021;21(1):160–177. doi:10.1016/j.spinee.2020.08.004
11. Guo JB, Che YJ, Hou JJ, et al. Stable mechanical environments created by a low-tension traction device is beneficial for the regeneration and repair of degenerated intervertebral discs. *Spine J*. 2020;20(9):1503–1516. doi:10.1016/j.spinee.2020.04.005
12. Zhan JW, Wang SQ, Feng MS, et al. Constant compression decreases vascular bud and VEGFA expression in a rabbit vertebral endplate ex vivo culture model. *PLoS One*. 2020;15(6):e0234747. doi:10.1371/journal.pone.0234747
13. DiStefano TJ, Illien-Jünger S, Iatridis JC. Homeostasis disrupted by strain mechanosensing. *Nat Biomed Eng*. 2019;3(12):951–952. doi:10.1038/s41551-019-0491-3

14. Li H, Tian L, Li J, et al. The roles of circRNAs in intervertebral disc degeneration: inflammation, extracellular matrix metabolism, and apoptosis. *Anal Cell Pathol*. 2022;2022:9550499. doi:10.1155/2022/9550499
15. Zhu H, Chen G, Wang Y, et al. Dimethyl fumarate protects nucleus pulposus cells from inflammation and oxidative stress and delays the intervertebral disc degeneration. *Exp Ther Med*. 2020;20(6):269. doi:10.3892/etm.2020.9399
16. Song Q, Zhang F, Wang K, et al. MiR-874-3p plays a protective role in intervertebral disc degeneration by suppressing MMP2 and MMP3. *Eur J Pharmacol*. 2021;895:173891. doi:10.1016/j.ejphar.2021.173891
17. Risbud MV, Shapiro IM. Role of cytokines in intervertebral disc degeneration: pain and disc content. *Nat Rev Rheumatol*. 2014;10(1):44–56. doi:10.1038/nrrheum.2013.160
18. Zhou Y, Chen Z, Yang X, et al. Morin attenuates pyroptosis of nucleus pulposus cells and ameliorates intervertebral disc degeneration via inhibition of the TXNIP/NLRP3/Caspase-1/IL-1β signaling pathway. *Biochem Biophys Res Commun*. 2021;559:106–112. doi:10.1016/j.bbrc.2021.04.090
19. Chen ZH, Jin SH, Wang MY, et al. Enhanced NLRP3, caspase-1, and IL- 1β levels in degenerate human intervertebral disc and their association with the grades of disc degeneration. *Anat Rec*. 2015;298(4):720–726. doi:10.1002/ar.23059
20. Chen F, Jiang G, Liu H, et al. Melatonin alleviates intervertebral disc degeneration by disrupting the IL-1β/NF-κB-NLRP3 inflammasome positive feedback loop. *Bone Res*. 2020;8:10. doi:10.1038/s41413-020-0087-2
21. He D, Zhou M, Bai Z, et al. Propionibacterium acnes induces intervertebral disc degeneration by promoting nucleus pulposus cell pyroptosis via NLRP3-dependent pathway. *Biochem Biophys Res Commun*. 2020;526(3):772–779. doi:10.1016/j.bbrc.2020.03.161
22. Nianhu L, Lei X, Sheng Y, et al. Effect of Bushenhuoxue formula on interleukin-1 beta and discoidin domain receptor 2 levels in a rat model of osteoarthritis. *J Tradit Chin Med*. 2015;35(2):192–196. doi:10.1016/S0254-6272(15)30027-3
23. Wang S, Xu S, Zhou J, et al. Luteolin transforms the polarity of bone marrow-derived macrophages to regulate the cytokine storm. *J Inflamm*. 2021;18(1):21. doi:10.1186/s12950-021-00285-5
24. Xu D, Jin H, Wen J, et al. Hydrogen sulfide protects against endoplasmic reticulum stress and mitochondrial injury in nucleus pulposus cells and ameliorates intervertebral disc degeneration. *Pharmacol Res*. 2017;117:357–369. doi:10.1016/j.phrs.2017.01.005
25. Liu W, Jin S, Huang M, et al. Duhuo jisheng decoction suppresses matrix degradation and apoptosis in human nucleus pulposus cells and ameliorates disc degeneration in a rat model. *J Ethnopharmacol*. 2020;250:112494. doi:10.1016/j.jep.2019.112494
26. Chen S, Wu X, Lai Y, et al. Kindlin-2 inhibits Nlrp3 inflammasome activation in nucleus pulposus to maintain homeostasis of the intervertebral disc. *Bone Res*. 2022;10(1):5. doi:10.1038/s41413-021-00179-5
27. Han B, Zhu K, Li FC, et al. A simple disc degeneration model induced by percutaneous needle puncture in the rat tail. *Spine*. 2008;33 (18):1925–1934. doi:10.1097/BRS.0b013e31817c64a9
28. Zhang B, Xu H, Wang J, et al. A narrative review of non-operative treatment, especially traditional Chinese medicine therapy, for lumbar intervertebral disc herniation. *Biosci Trends*. 2017;11(4):406–417. doi:10.5582/bst.2017.01199
29. Zhu L, Yu C, Zhang X, et al. The treatment of intervertebral disc degeneration using traditional Chinese medicine. *J Ethnopharmacol*. 2020;263:113117. doi:10.1016/j.jep.2020.113117
30. Ma YM, Zhang XZ, Su ZZ, et al. Insight into the molecular mechanism of a herbal injection by integrating network pharmacology and in vitro. *J Ethnopharmacol*. 2015;173:91–99. doi:10.1016/j.jep.2015.07.016
31. Wang S, Cao M, Xu S, et al. Luteolin alters macrophage polarization to inhibit inflammation. *Inflammation*. 2020;43(1):95–108.
32. Caporali S, De Stefano A, Calabrese C, et al. Anti-inflammatory and active biological properties of the plant-derived bioactive compounds luteolin and luteolin 7-glucoside. *Nutrients*. 2022;14(6):1155. doi:10.3390/nu14061155
33. Yu H, Hou G, Cao J, et al. Mangiferin alleviates mitochondrial ROS in nucleus pulposus cells and protects against intervertebral disc degeneration via suppression of NF-κB signaling pathway. *Oxid Med Cell Longev*. 2021;2021:6632786. doi:10.1155/2021/6632786
34. Ma H, Xie C, Chen Z, et al. MFG-E8 alleviates intervertebral disc degeneration by suppressing pyroptosis and extracellular matrix degradation in nucleus pulposus cells via Nrf2/TXNIP/NLRP3 axis. *Cell Death Discov*. 2022;8(1):209. doi:10.1038/s41420-022-01002-8
35. Sinha K, Das J, Pal PB, et al. Oxidative stress: the mitochondria-dependent and mitochondria-independent pathways of apoptosis. *Arch Toxicol*. 2013;87(7):1157–1180. doi:10.1007/s00204-013-1034-4
36. Zheng Z, Wang ZG, Chen Y, et al. Spermidine promotes nucleus pulposus autophagy as a protective mechanism against apoptosis and ameliorates disc degeneration. *J Cell Mol Med*. 2018;22(6):3086–3096. doi:10.1111/jcmm.13586
37. Zhang F, Liu Z, He X, et al. β-Sitosterol-loaded solid lipid nanoparticles ameliorate complete Freund's adjuvant-induced arthritis in rats: involvement of NF-κB and HO-1/Nrf-2 pathway. *Drug Deliv*. 2020;27(1):1329–1341. doi:10.1080/10717544.2020.1818883
38. Bilia AR, Piazzini V, Guccione C, et al. Improving on nature: the role of nanomedicine in the development of clinical natural drugs. *Planta Med*. 2017;83(5):366–381. doi:10.1055/s-0043-102949
39. Li W, Zhang Y, Xing C, et al. Tanshinone IIA represses inflammatory response and reduces radiculopathic pain by inhibiting IRAK-1 and NF-κB/p38/JNK signaling. *Int Immunopharmacol*. 2015;28(1):382–389. doi:10.1016/j.intimp.2015.06.032
40. Dai S, Shi X, Qin R, et al. Sodium tanshinone IIA sulfonate ameliorates injury-induced oxidative stress and intervertebral disc degeneration in rats by inhibiting p38 MAPK signaling pathway. *Oxid Med Cell Longev*. 2021;2021:5556122. doi:10.1155/2021/5556122
41. Ryoo IG, Kwak MK. Regulatory crosstalk between the oxidative stress-related transcription factor Nfe2l2/Nrf2 and mitochondria. *Toxicol Appl Pharmacol*. 2018;359:24–33. doi:10.1016/j.taap.2018.09.014
42. Kang L, Liu S, Li J, et al. Parkin and Nrf2 prevent oxidative stress-induced apoptosis in intervertebral endplate chondrocytes via inducing mitophagy and anti-oxidant defenses. *Life Sci*. 2020;243:117244. doi:10.1016/j.lfs.2019.117244
43. Du X, Wang X, Cui K, et al. Tanshinone IIA and astragaloside IV inhibit miR-223/JAK2/STAT1 signalling pathway to alleviate lipopolysaccharide-induced damage in nucleus pulposus cells. *Dis Markers*. 2021;2021:6554480. doi:10.1155/2021/6554480
44. Zhang HJ, Ma XH, Xie SL, et al. Knockdown of miR-660 protects nucleus pulposus cells from TNF-a-induced apoptosis by targeting serum amyloid A1. *J Orthop Surg Res*. 2020;15(1):7. doi:10.1186/s13018-019-1538-6
45. Wang K, Chen T, Ying X, et al. Ligustilide alleviated IL-1β induced apoptosis and extracellular matrix degradation of nucleus pulposus cells and attenuates intervertebral disc degeneration in vivo. *Int Immunopharmacol*. 2019;69:398–407. doi:10.1016/j.intimp.2019.01.004
46. Luo Z, Ma Y, Di T, et al. DNMT3B decreases extracellular matrix degradation and alleviates intervertebral disc degeneration through TRPA1 methylation to inhibit the COX2/YAP axis. *Aging*. 2021;13(16):20258–20276. doi:10.18632/aging.203410